

## Electronic Supplementary Information

### Regulation of carbon content in MOF-derived hierarchical-porous NiO@C films for high-performance electrochromic

Hao Liang,<sup>a</sup> Ran Li,<sup>a</sup> Ce Li,<sup>c</sup> Chengyi Hou,<sup>\*a</sup> Yaogang Li,<sup>\*b</sup> Qinghong Zhang<sup>b</sup> and Hongzhi Wang<sup>a</sup>

---

<sup>a</sup>. State Key Laboratory for Modification of Chemical Fibers and Polymer Materials, College of Materials Science and Engineering, Donghua University, Shanghai 201620, P. R. China. E-mail: [hcy@dhu.edu.cn](mailto:hcy@dhu.edu.cn)

<sup>b</sup>. Engineering Research Center of Advanced Glasses Manufacturing Technology, Ministry of Education, Donghua University, Shanghai 201620, P. R. China. E-mail: [yaogang\\_li@dhu.edu.cn](mailto:yaogang_li@dhu.edu.cn)

<sup>c</sup>. College of Mechanical Engineering, Donghua University, Shanghai 201620, P. R. China.

Keywords: electrochromic, metal-organic framework, nickel oxide, thermolysis, carbon

## Contents

Supplementary discussion.....	3
S1. Thermogravimetric analysis.....	3
S2. Calculation process of $D_w$ and $D_{CV}$ .....	3
Supplementary Figures.....	3
Fig. S1 TGA traces of Ni@C and Ni-MOF.....	3
Fig. S2 Cross-sectional SEM images of Ni-MOF, Ni@C and hierarchical-porous NiO@C films.....	4
Fig. S3 SEM images of A-10, A-30 and A-60 films.....	4
Fig. S4 HRTEM image of Ni@C.....	4
Fig. S5 Raman spectrum of Ni@C and hierarchical-porous NiO@C .....	5
Fig. S6 TEM images of A-10, A-30 and A-60.....	5
Fig. S7 Elemental mapping of A-10, A-30 and A-60.....	6
Fig. S8 X-ray photoelectron spectroscopy (XPS) of different films.....	6
Fig. S9 Digital photographs of HA-25 film electrode at different states.....	7
Fig. S10 Schematic illustration for HA-25-based number “6” film.....	7
Fig. S11 In situ transmittance responses (at 550 nm) for HA-20 and HA-30 films in 1 M KOH solution measured between 0 and 0.6 V bias.....	7
Fig. S12 In situ transmittance responses (at 550 nm) for A-10, A-30 and A-60 films in 1 M KOH solution measured between 0 and 0.6 V bias.....	8
Fig. S13 The Nyquist plots and corresponding simulation results (fitting lines) for HA-20 and HA-30 films measured in 1 M KOH solution.....	8
Fig. S14 The Nyquist plots and corresponding simulation results (fitting lines) for A-10 and A-30 films measured in 1 M KOH solution.....	8
Fig. S15 Cyclic voltammogram curves of different films.....	9
Fig. S16 Coloration efficiency of HA-20 and HA-30 films in 1 M KOH solution.....	10
Fig. S17 Coloration efficiency of A-10 and A-30 films in 1 M KOH solution.....	10
Supplementary Tables.....	11
Table S1 Percentage of each element of different NiO@C films from X-ray photoelectron spectroscopy (XPS).....	11
Table S2 Fitted parameters according to electrochemical impedance spectroscopy of different NiO@C films.....	11

Table S3 Comparison of $D_w$ and $D_{cv}$ for different NiO@C films.....	12
Table S4 Comparison of EC performances of NiO and other inorganic EC materials.....	12
Supplementary Movies.....	12
Supplementary references.....	13

## Supplementary discussion

### S1. Thermogravimetric analysis:

As shown in Fig. S1, the TGA trace of Ni@C shows a trend of increases initially and decreases afterwards. The weight gain from 290 °C to 390 °C owing to the process of metal oxidation; The followed weight loss after 390 °C because of the carbon decomposition.

For Ni-MOF: The first weight loss (about 5%) before 200 °C due to the volatilization of embedded solvent molecules; Then the second weight loss (about 50%) from 340 °C to 390 °C related to the rapid decomposition of Ni-MOF.

### S2. Calculation process of $D_w$ and $D_{cv}$ :

#### Calculation process for $D_w$ according to the equation S1 (Fick's law).

$$D_w = R^2 T^2 / 2S^2 n^4 F^4 C^2 \sigma^2 \quad (S1)$$

Where R is the gas constant, T is the absolute temperature, S is the effective working area, F is the Faraday constant, n is the number of electrons, C is molar concentrations of ions and  $\sigma$  represents the Warburg constant.

#### Calculation process for $D_{cv}$ according to the equation S2 (Randles–Sevcik equation).

$$i_p = 2.687 \times 10^5 \times n^{3/2} \times D_{cv}^{1/2} \times C \times S \times v^{1/2} \quad (S2)$$

In the above equation,  $i_p$  is the peak current density, n is the number of electrons, C is the concentration of active  $\text{OH}^-$  ions, S is the surface area and v is the potential sweep rate.

## Supplementary Figures

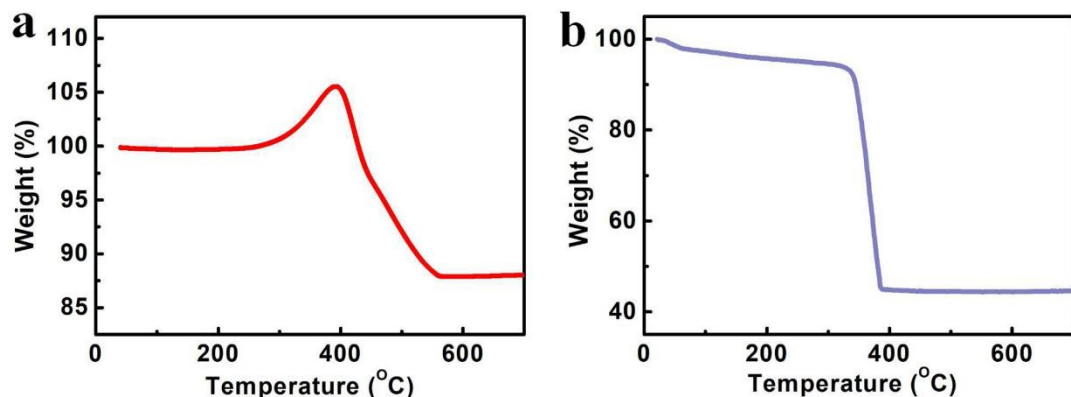


**Fig. S1** TGA traces of (a) Ni@C powder, (b) Ni-MOF powder at the heating rate of 10 °C/ min in air atmosphere.

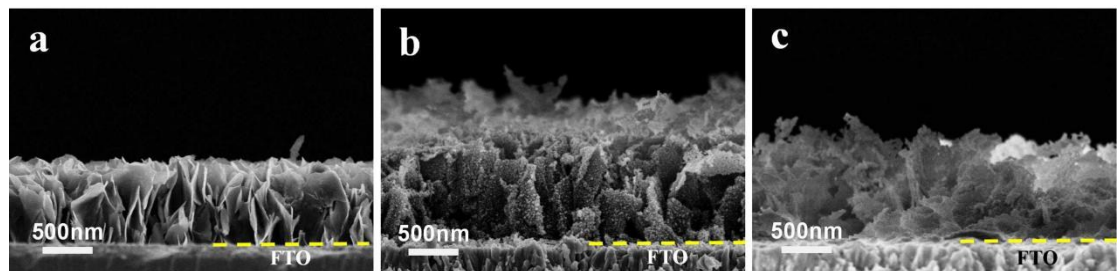


**Fig. S2** Cross-sectional SEM images of (a) Ni-MOF, (b) Ni@C and (c) hierarchical-porous NiO@C layer on FTO glass.

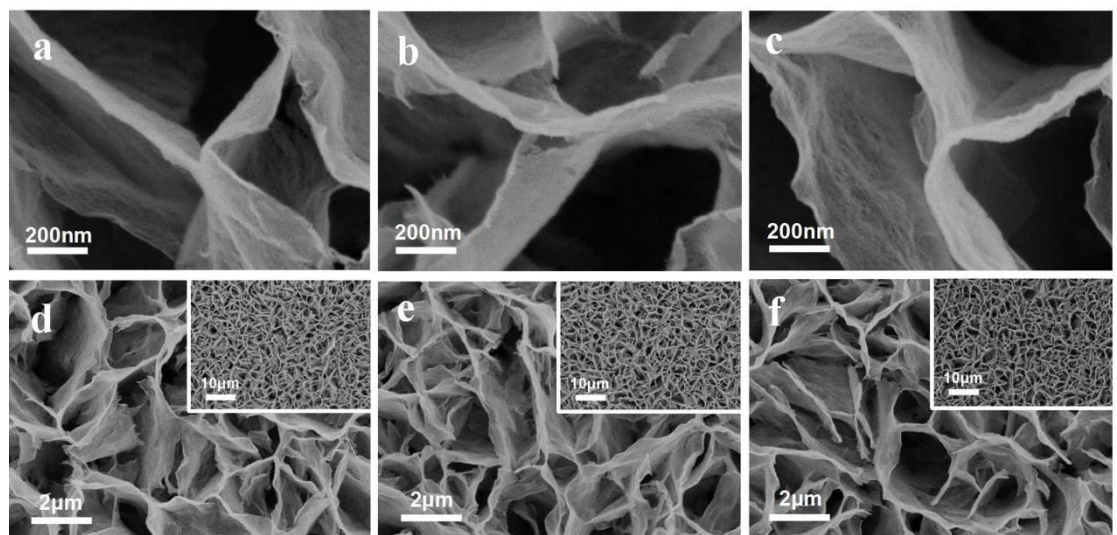


**Fig. S3** SEM images of (a, d) A-10, (b, e) A-30 and (c, f) A-60 films.

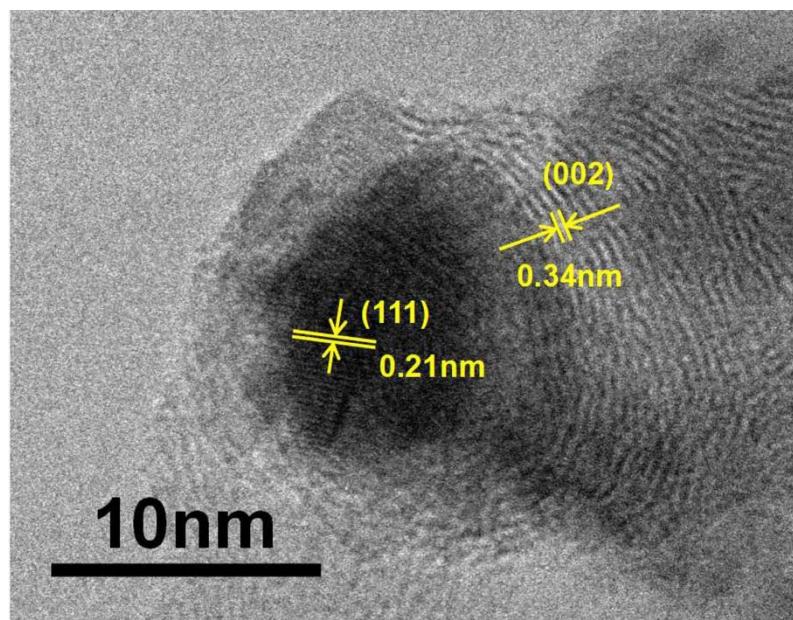


**Fig. S4** HRTEM image of Ni@C.

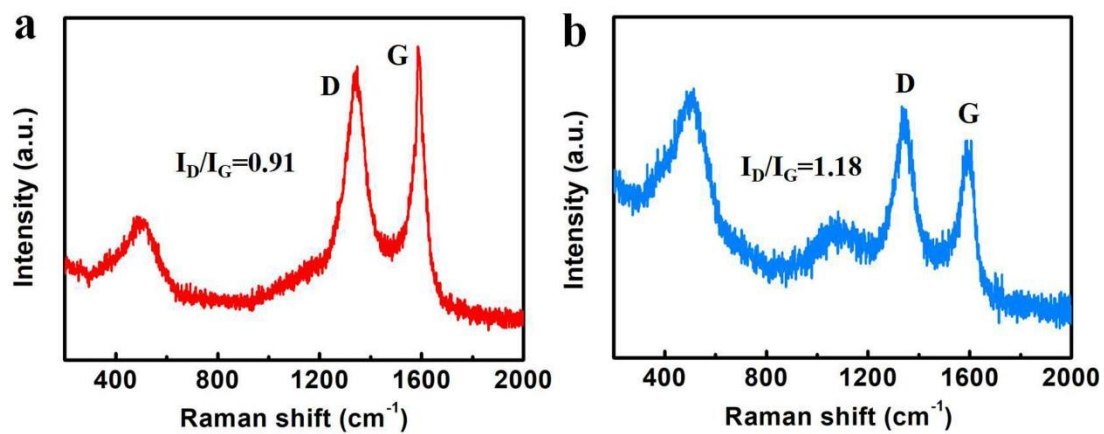


**Fig. S5** Raman spectrum of (a) Ni@C and (b) hierarchical-porous NiO@C.

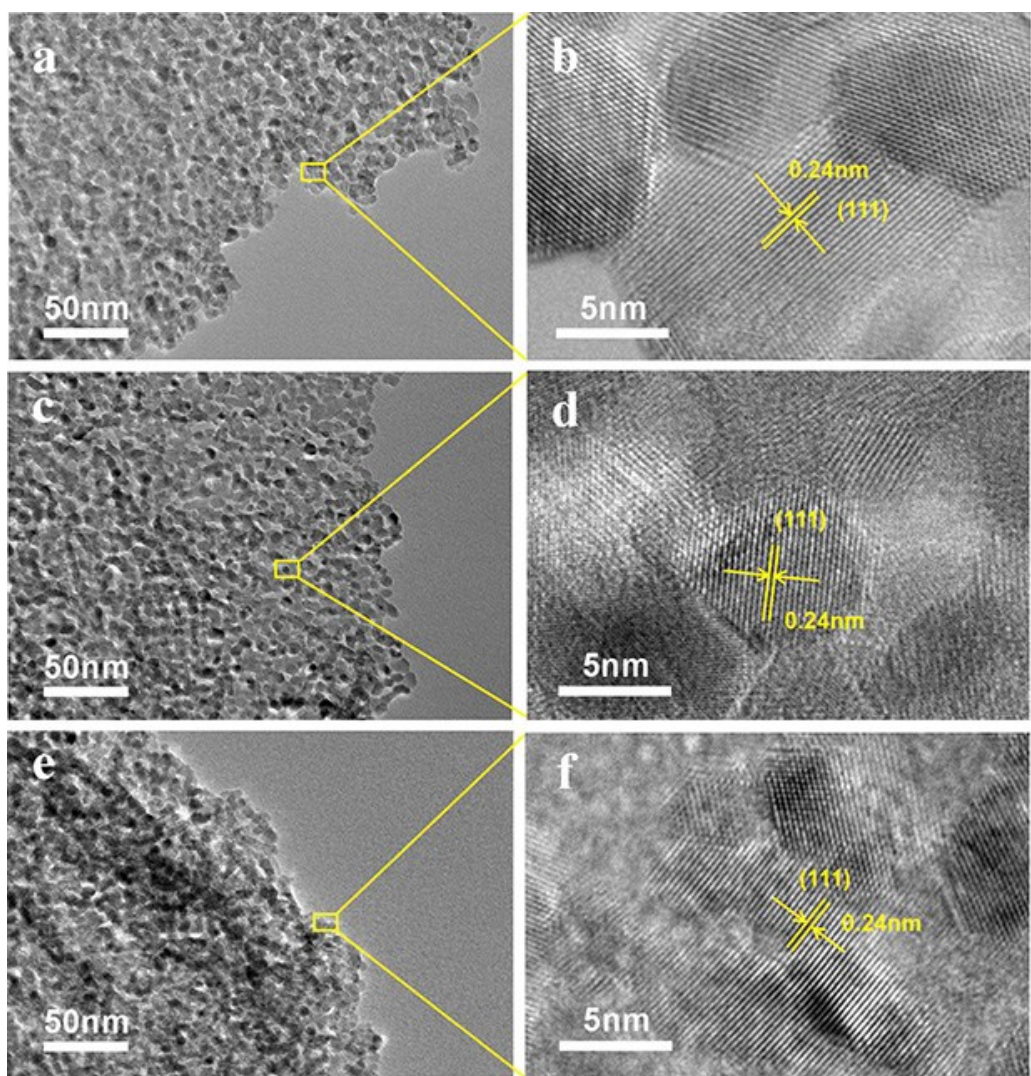


**Fig. S6** TEM images of (a, b) A-10, (c, d) A-30 and (e, f) A-60.

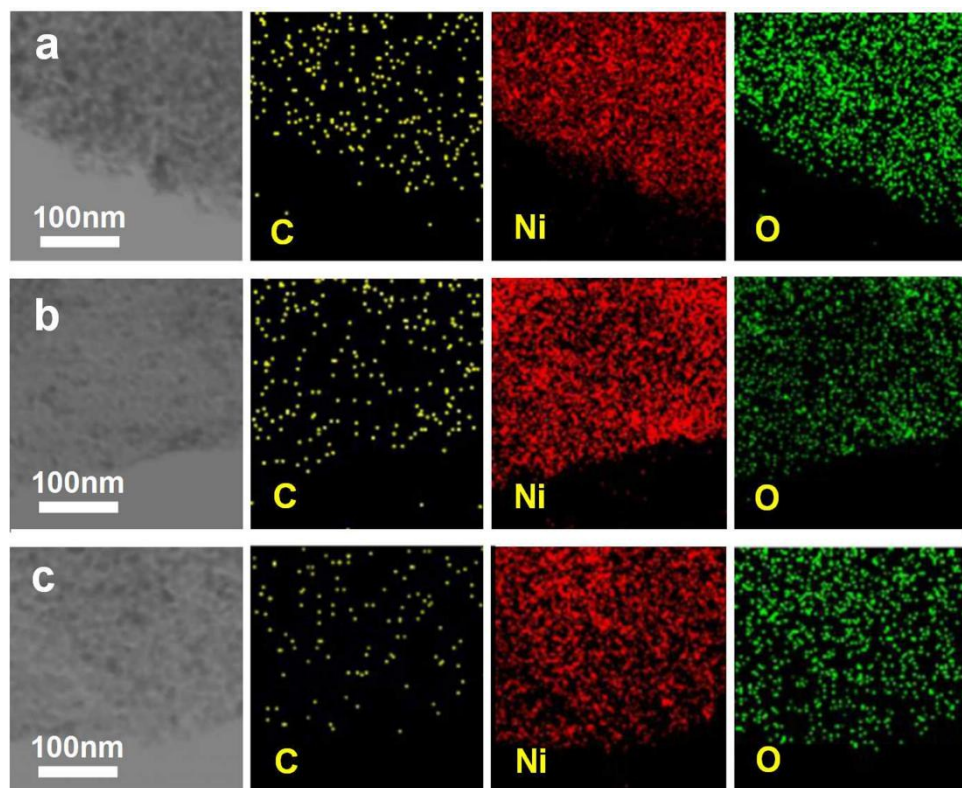


**Fig. S7** Elemental mapping of (a) A-10, (b) A-30 and (c) A-60.

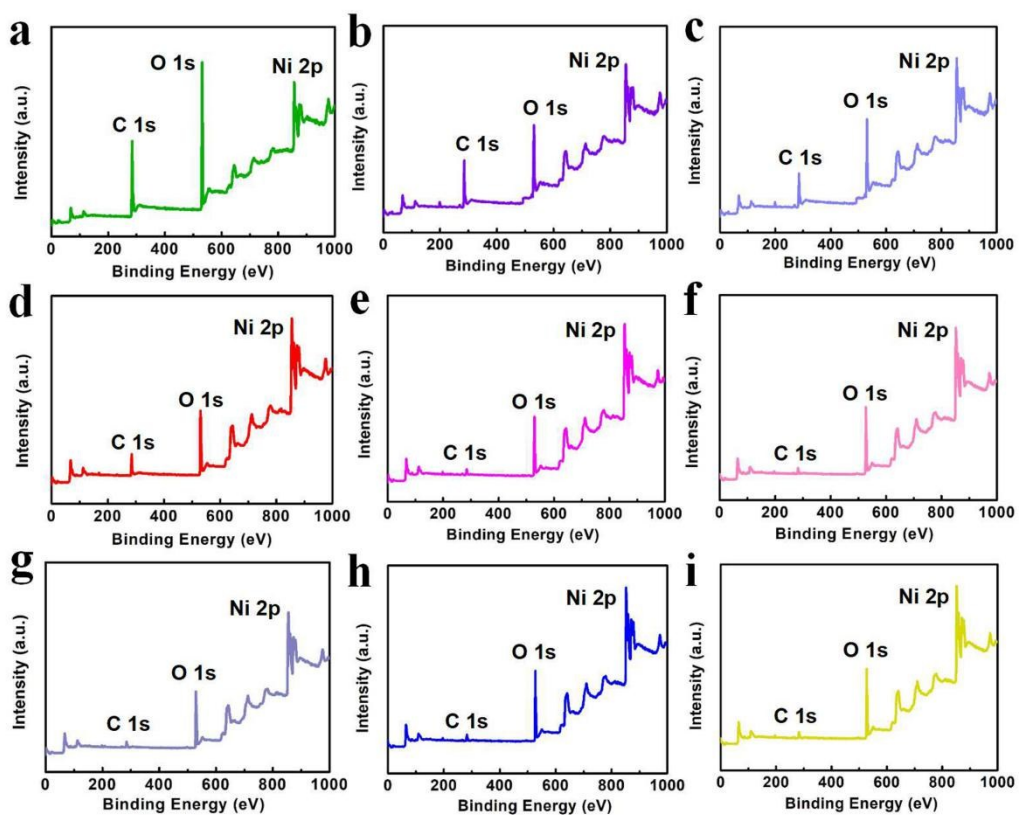


**Fig. S8** X-ray photoelectron spectroscopy (XPS) of (a) PTA-Ni-MOF; (b) HA-15; (c) HA-20; (d) HA-25; (e) HA-30; (f) HA-60; (g) A-10; (h) A-30 and (i) A-60.

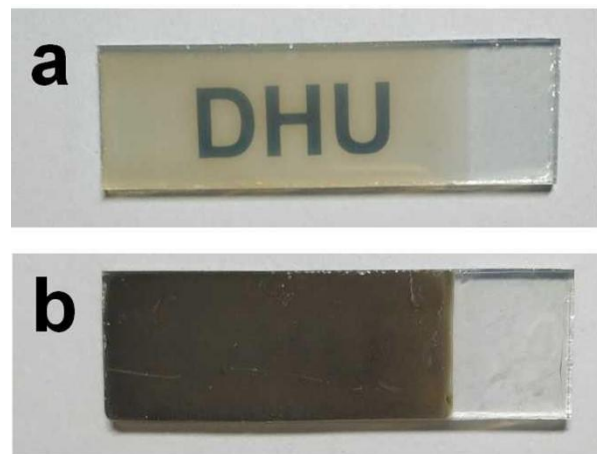


**Fig. S9** Digital photographs of HA-25 film electrode at (a) bleached state and (b) colored state.

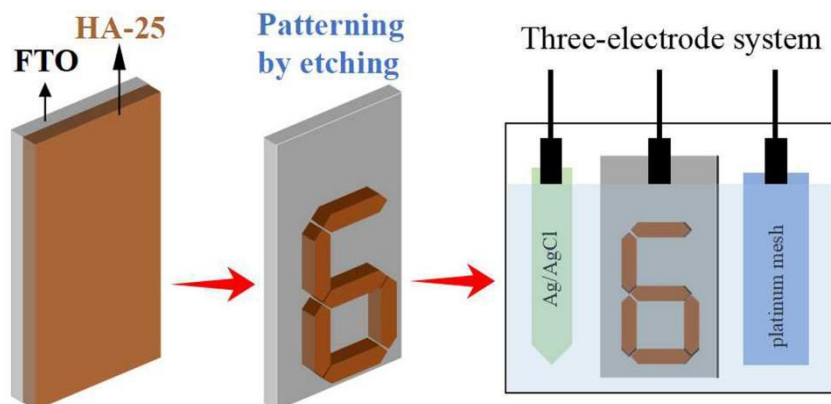


**Fig. S10** Schematic illustration for HA-25-based number “6” film.

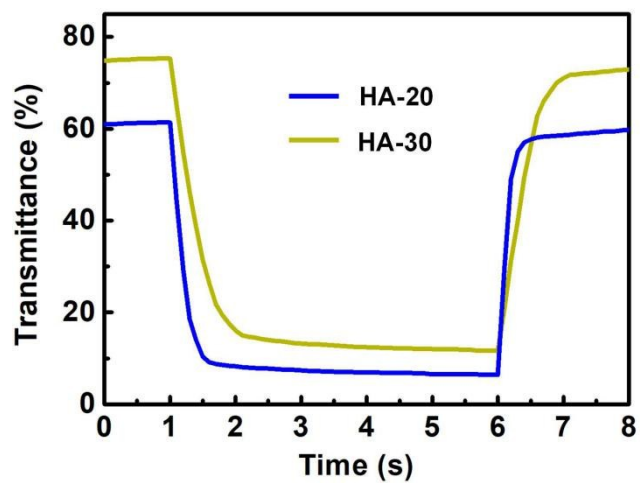


**Fig. S11** In situ transmittance responses (at 550 nm) for HA-20 and HA-30 films in 1 M KOH solution measured between 0 and 0.6 V bias.

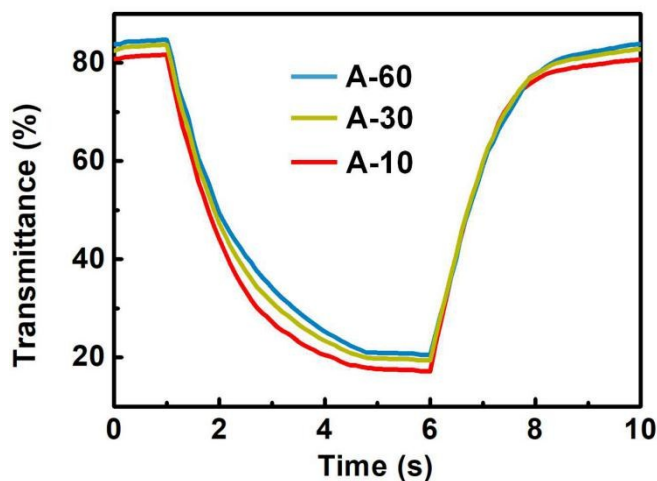


**Fig. S12** In situ transmittance responses (at 550 nm) for A-10, A-30 and A-60 films in 1 M KOH solution measured between 0 and 0.6 V bias.

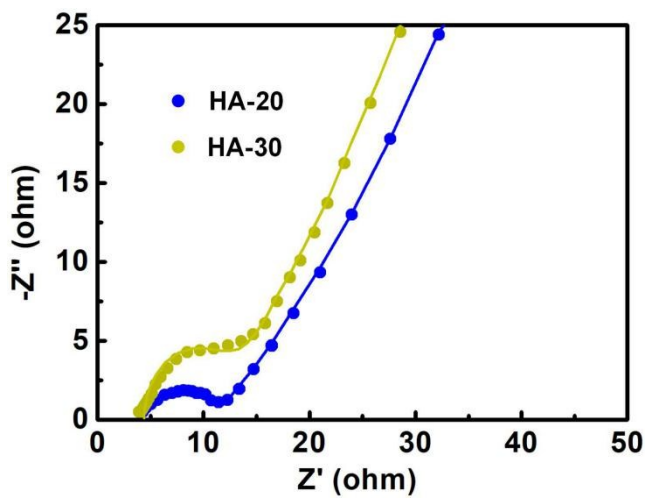


**Fig. S13** The Nyquist plots and corresponding simulation results (fitting lines) for HA-20 and HA-30 films measured in 1 M KOH solution.

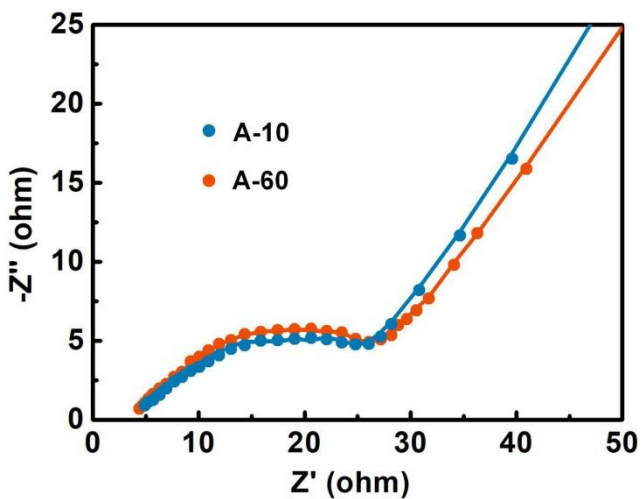


**Fig. S14** The Nyquist plots and corresponding simulation results (fitting lines) for A-10 and A-30 films measured in 1 M KOH solution.

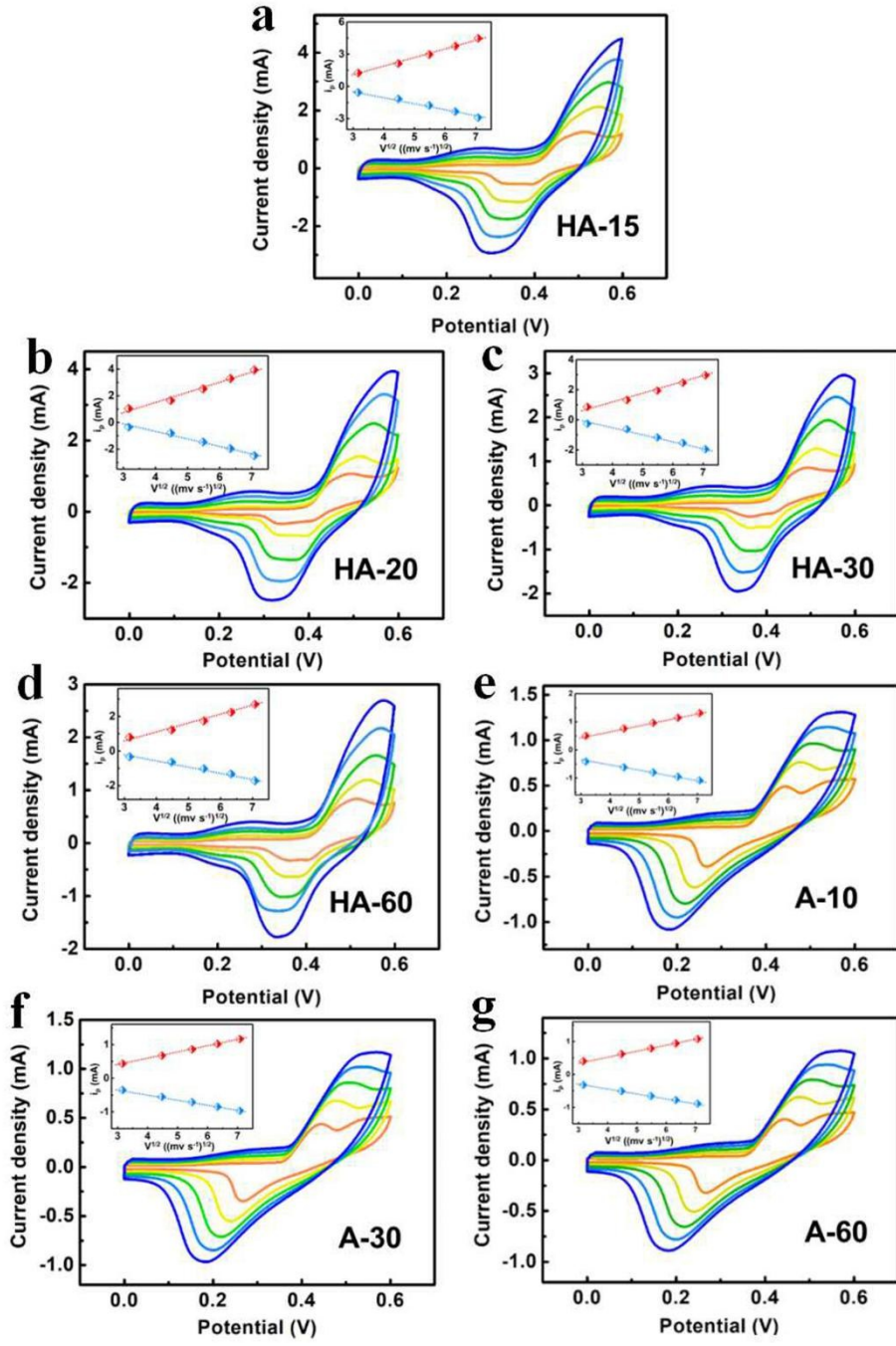


**Fig. S15** Cyclic voltammogram curves of (a) HA-15; (b) HA-20; (c) HA-30; (d) HA-60; (e) A-10; (f) A-30 and (g) A-60 films measured in 1M KOH solution. Scan rates: 10, 20, 30, 40 and 50 mV/s.

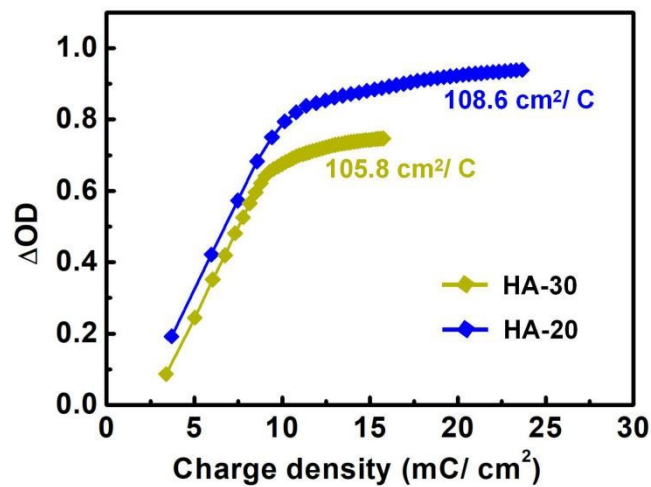


**Fig. S16** Coloration efficiency of HA-20 and HA-30 films in 1 M KOH solution.

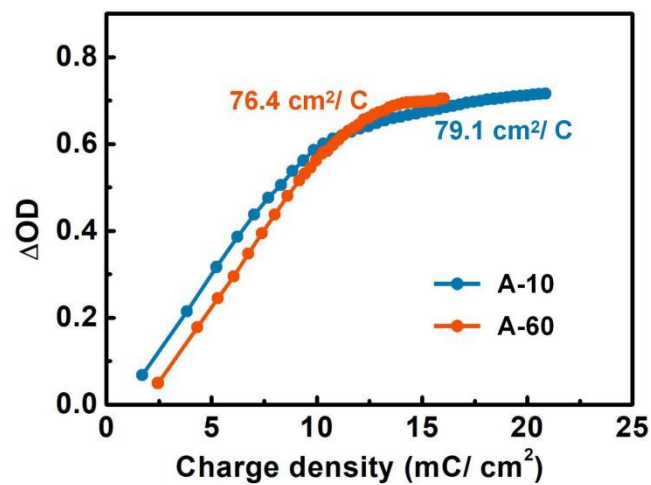


**Fig. S17** Coloration efficiency of A-10 and A-30 films in 1 M KOH solution.

## Supplementary Tables

**Table S1** Percentage of each element of different NiO@C films from X-ray photoelectron spectroscopy (XPS).

Films	Atomic% (C)	Atomic% (O)	Atomic% (Ni)
HA-15	29.74	39.51	30.75
HA-20	19.15	43.59	37.26
HA-25	11.42	46.44	42.13
HA-30	6.01	47.97	46.02
HA-60	3.96	48.54	47.5
A-10	5.05	47.36	47.59
A-30	4.42	48.03	47.55
A-60	3.77	48.62	47.61

**Table S2** Fitted parameters according to electrochemical impedance spectroscopy of different NiO@C films.

Films	R <sub>s</sub> ( $\Omega$ )	R <sub>ct</sub> ( $\Omega$ )	$\sigma$ ( $\Omega \times s^{-1/2}$ )
HA-15	4.03	4.24	38.65
HA-20	4.11	6.82	42.50
HA-25	4.26	7.59	45.90
HA-30	4.40	12.51	48.16
HA-60	4.49	15.36	51.09

A-10	4.67	42.65	113.53
A-30	4.75	45.14	118.69
A-60	4.81	45.78	123.04

**Table S3** Comparison of  $D_w$  of different NiO@C films calculated from Fick's law and  $D_{cv}$  calculated from Randles–Sevcik equation.

Films	$D_w$ calculated from Fick's law ( $\text{cm}^2/\text{s}$ )	$D_{cv}$ calculated from R–S equation ( $\text{cm}^2/\text{s}$ )
HA-15	$1.85 \times 10^{-7}$	$1.37 \times 10^{-7}/2.94 \times 10^{-8}$
HA-20	$1.53 \times 10^{-7}$	$1.08 \times 10^{-7}/2.55 \times 10^{-8}$
HA-25	$1.31 \times 10^{-7}$	$9.72 \times 10^{-8}/1.76 \times 10^{-8}$
HA-30	$1.19 \times 10^{-7}$	$9.55 \times 10^{-8}/1.57 \times 10^{-8}$
HA-60	$1.06 \times 10^{-7}$	$9.08 \times 10^{-8}/1.44 \times 10^{-8}$
A-10	$2.14 \times 10^{-8}$	$1.21 \times 10^{-8}/7.73 \times 10^{-9}$
A-30	$1.97 \times 10^{-8}$	$9.93 \times 10^{-9}/7.12 \times 10^{-9}$
A-60	$1.82 \times 10^{-8}$	$9.64 \times 10^{-9}/6.89 \times 10^{-9}$

**Table S4** Comparison of EC performances of NiO and other inorganic EC materials.

EC materials	Coloring/bleaching time	CE	Cycling stability	Reference
NiO	7.2/6.7 s	$76 \text{ cm}^2 \text{ C}^{-1}$	2200 cycles	1

NiO	~5 s	88 cm <sup>2</sup> C <sup>-1</sup>	NA	2
NiO	< 0.1 s	~45 cm <sup>2</sup> C <sup>-1</sup>	1000 cycles	3
WO <sub>3</sub>	5.8/1 s	51.4 cm <sup>2</sup> C <sup>-1</sup>	81.6% after 1000 cycles	4
WO <sub>3</sub>	0.93/1.27s	71.8 cm <sup>2</sup> C <sup>-1</sup>	450 cycles	5
WO <sub>3-x</sub>	0.9/1 s	154 cm <sup>2</sup> C <sup>-1</sup>	NA	6
Ni/Mg-NDISA	~7 s	~100 cm <sup>2</sup> C <sup>-1</sup>	NA	7
<b>This work</b>	<b>0.46/0.25 s</b>	<b>113.5 cm<sup>2</sup> C<sup>-1</sup></b>	<b>90.1% after 20000 cycles</b>	

## Supplementary Movies

**Movie S1** HA-25 film measured in three electrode system powered by electrochemical workstation.

**Movie S2** Digital display device powered by commercial batteries.

## Supplementary References

- 1 G.-F. Cai, J.-P. Tu, J. Zhang, Y.-J. Mai, Y. Lu, C.-D. Gu and X.-L. Wang, *Nanoscale*, 2012, **4**, 5724-5730.
- 2 D. S. Dalavi, R. S. Devan, R. S. Patil, Y. R. Ma, M. G. Kang, J. H. Kim and P. S. Patil, *J. Mater. Chem. A.*, 2013, **1**, 1035-1039.
- 3 M. R. J. Scherer and U. Steiner, *Nano Lett.*, 2013, **13**, 3005-3010.
- 4 B.-R. Koo and H.-J. Ahn, *Nanoscale*, 2017, **9**, 17788-17793.
- 5 Z. Q. Xie, Q. Q. Zhang, Q. Q. Liu, J. Zhai and X. G. Diao, *Thin Solid Films*, 2018, **653**, 188-193.
- 6 S. Cong, Y. Y. Tian, Q. W. Li, Z. G. Zhao, F. X. Geng, *Adv. Mater.*, 2014, **26**, 4260-4267.
- 7 K. AlKaabi, C. R. Wade and M. Dincă, *Chem.*, 2016, **1**, 264-272.